Reactions of Di- and Polynuclear Complexes. 10.[1] Carbonyl Substitution of $[Fe_2(CO)_6\{\mu\text{-}C_2(CF_3)_2S\}]$ with Phosphorus Ligands: Kinetics and Mechanisms. Fluxional Behavior of These Diiron Compounds and Related Complexes

René Rumin, Françoise Robin-Le Guen, François Y. Pétillon,* Roger Pichon, and Jean Talarmin

URA CNRS No. 322, "Chimie, Electrochimie Moléculaires et Chimie Analytique", Faculté des Sciences, Université de Bretagne Occidentale, B.P. 452, 29275 Brest Cedex, France

Received December 9, 1992

The reaction of the diiron complex $[Fe_2(CO)_6\{\mu\text{-}C_2(CF_3)_2S\}]$ (1) with trimethyl phosphite and diphosphines ($PPh_2(CH_2)_xPPh_2$: x = 1 (dppm), 2 (dppe)) proceeds readily to form monosubstituted products. A second substitution is observed for trimethyl phosphite and diphosphines. The reaction follows a second-order process when $P(OMe)_3$ replaces one and two carbonyl ligands. A mechanism for the substitution reactions is proposed. The fluxional behavior of the cluster 1 and of its substituted derivatives $[Fe_2(CO)_{6-x}L_x\{\mu\text{-}C_2(CF_3)_2S\}]$ (x = 1, L = $P(OMe)_3$ (2), dppm (7), dppe (12); x = 2, L = $P(OMe)_3$ (3), $P(OMe)_3$ and PMe_3 (4), dppe (14); x = 3, L = $P(OMe)_3$ (5)) have been investigated by variable-temperature ^{13}C, ^{19}F, and ^{31}P NMR spectroscopy. Two main processes have been established. The local scramblings have been identified and the relevant mechanisms discussed.

Introduction

Ligand substitution on transition-metal carbonyl compounds is a subject of active interest with respect to homogeneous and heterogeneous catalysis.[2] Substitution of CO ligands is generally effected under thermal and photochemical conditions and often leads to a mixture of mono- and polysubstituted complexes; under electrochemical activation specific replacement of carbon monoxide by other ligands is observed.[3] Thermal substitution reactions in even-electron organometallic systems may occur via two typical pathways:[4] (a) associative for 16-electron compounds; (b) dissociative for 18-electron compounds. In organometallic substitution reactions a ligand may change the mechanism through variable bonding capabilities, as shown by nitrosyl,[5] carbonyl,[6] and η^5-cyclopentadienyl[6a,7] complexes. The substitution reactions of 18-electron polynuclear complexes, involving a simple replacement of a neutral two-electron ligand by a more basic one, may proceed by an associative mechanism owing to the participation of ancillary bridging ligands. Such a mechanism implies partial and temporary decoordination of polyhapto ligands and then delocalization of a pair of electrons from the metal complex onto one of its ligands, making a vacant low-energy orbital available on the metal to permit nucleophilic attack.[6a,8]

We have reported previously a study[1] of replacement of carbon monoxide by trimethyl phosphite, phosphines, and diphosphines in $[Fe_2(CO)_6\{\mu\text{-}C_2(CF_3)_2S\}]$ (1) and related compounds (Chart I) under thermal, photochemical, and electrochemical activation. On the basis of the above considerations, it was interesting to examine the mechanism of ligand substitution for this class of compounds. We report here the kinetic results of our investigation on the CO replacement reactions in 1 and $[Fe_2(CO)_5\{P(OMe)_3\}\{\mu\text{-}C_2(CF_3)_2S\}]$ (2). Also reported here, and of equal interest, are the variable-temperature NMR (^{13}C, ^{19}F, ^{31}P) spectra of 1 and related clusters that indicate a number of different fluxional processes occur in each molecule in solution. The mode of collapse of the signals in the highest energy process of 1 and 2 is consistent with iron–carbon bond breaking. This involves the creation of a vacant coordination site, providing a rationale as to how these coordinatively saturated organometallic compounds may react by an associative mechanism.

Results

Kinetic Analysis. 1. Reaction of $[Fe_2(CO)_6\{\mu\text{-}C_2(CF_3)_2S\}]$ (1) with $P(OMe)_3$. Rates for the reaction (eq 1) of 1 (0.17 M) in toluene-d_8 with a stoichiometric amount of $P(OMe)_3$ were calculated by monitoring the time dependence of the ^{19}F NMR spectra of either the starting material or of the products, at five temperatures. Both monosubstituted isomers **2a,b** are formed in the early stage of the reaction: at longer times disubstituted products are observed. Thus, clusters 2 undergo further substitution to give the disubstituted complex $[Fe_2(CO)_4\{P(OMe)_3\}_2\{\mu\text{-}C_2(CF_3)_2S\}]$ (**3**). The rate of disappearance of the diiron starting complex 1 was fitted to a second-order rate law.

(1) Part 9: Robin, F.; Rumin, R.; Talarmin, J.; Pétillon, F. Y.; Muir, K. W. *Organometallics* **1993**, *12*, 365.
(2) Basolo, F. *Coord. Chem. Rev.* **1990**, *100*, 47.
(3) (a) Darchen, A.; Mahé, C.; Patin, H. *New J. Chem.* **1982**, *6*, 539. (b) Ohst, H. H.; Kochi, J. K. *J. Am. Chem. Soc.* **1986**, *108*, 2897. (c) Pétillon, F. Y.; Rumin, R.; Talarmin, J. *J. Organomet. Chem.* **1988**, *346*, 111. (d) Arewgoda, M.; Robinson, B. H.; Simpson, J. *J. Chem. Soc., Chem. Commun.* **1982**, 284. (e) Astruc, D. *Angew. Chem., Int. Ed. Engl.* **1988**, *27*, 643.
(4) (a) Langford, C. H.; Gray, H. B. In *Ligand Substitution Processes*; Benjamin, W. A., Ed.; New York, 1965. (b) Tolman, C. A. *Chem. Soc. Rev.* **1972**, *1*, 337. (c) Darensbourg, D. J. *Adv. Organomet. Chem.* **1982**, *21*, 113.
(5) Dobson, G. R. *Acc. Chem. Res.* **1976**, *9*, 300.
(6) (a) Basolo, F. *Inorg. Chim. Acta* **1985**, *100*, 33. (b) Wang, J. Q.; Shen, J. K.; Gao, Y. C.; Shi, Q. Z.; Basolo, F. *J. Organomet. Chem.* **1991**, *417*, 131.
(7) Kershner, D. L.; Basolo, F. *J. Am. Chem. Soc.* **1987**, *109*, 7396.
(8) Darchen, A.; Lhadi, E. K.; Patin, H. *J. Organomet. Chem.* **1989**, *363*, 137.

0276-7333/93/2312-1597$04.00/0

Chart I

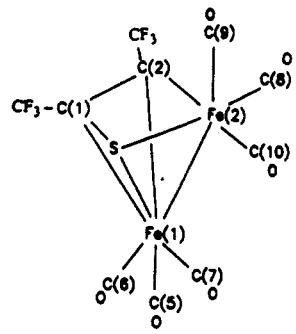

1

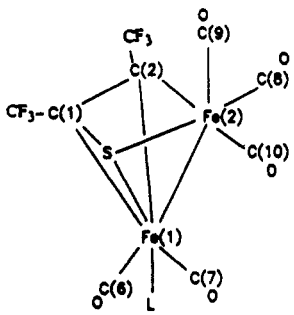

2a

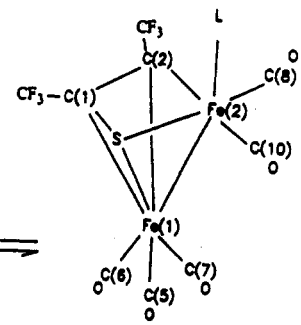

2b

2 L = P(OMe)$_3$

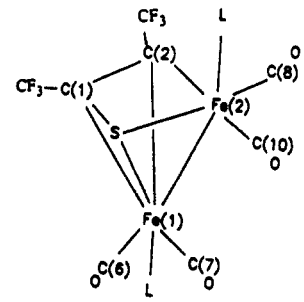

3 L = P(OMe)$_3$

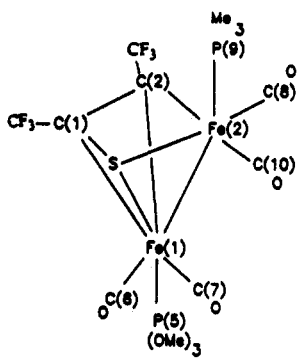

4a

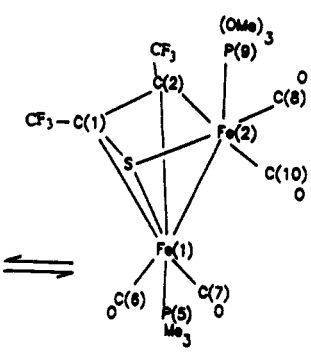

4b

4

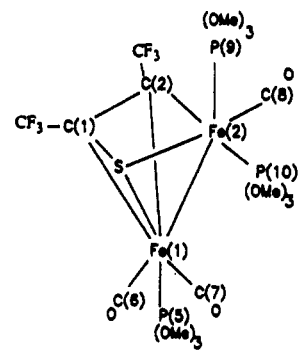

5 a

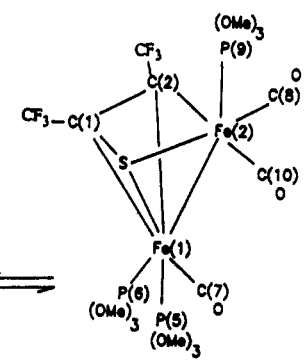

5 b

5

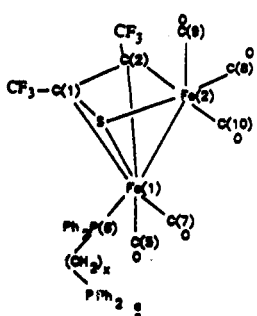

6

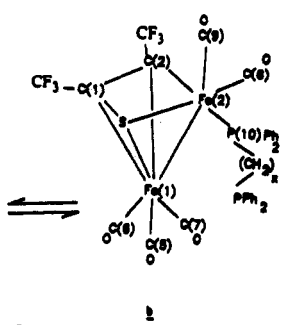

7 x=1 dppm

12 x=2 dppe

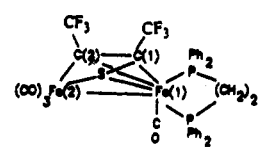

14 a

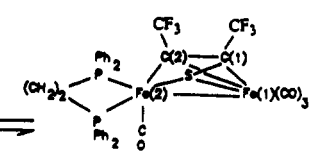

14 b

14

This can be seen from the linear plots (in all five cases) of $100/(100-x)$ (where x is the percentage of the product 2) vs time (Figure 1): k was obtained from the slopes of such plots. In this case, only data from the early stage of

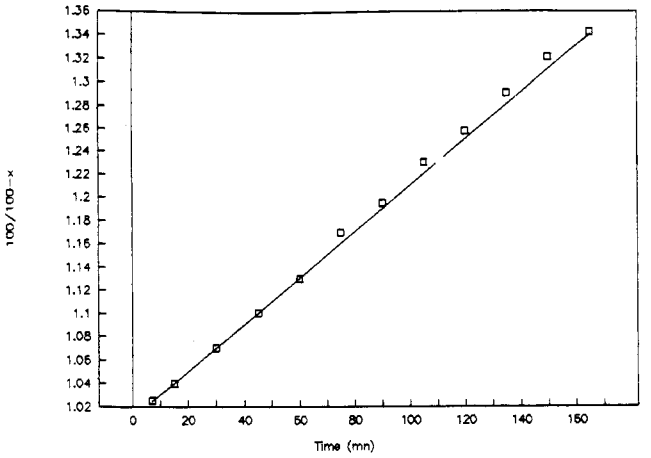

Figure 1. Second-order kinetics observed in the thermal CO substitution of 1 (0.17 M) in toluene-d_8 containing 0.17 M $P(OMe)_3$ at 378 K.

$$[Fe_2(CO)_6\{\mu\text{-}C_2(CF_3)_2S\}] + P(OMe)_3 \rightarrow \underset{\mathbf{1}}{} \quad [Fe_2(CO)_5\{P(OMe)_3\}\{\mu\text{-}C_2(CF_3)_2S\}] + CO \quad (1)$$
$$\mathbf{2a,b}$$

the reaction were used. The rate constants for the disappearance of 1 are given in Table I. The linear Eyring plot of the exchange rate constant in Figure 2 afforded the activation parameters $\Delta H^{\ddagger} = 31.5$ (±1.5) kcal mol^{-1} and $\Delta S^{\ddagger} = 6.8$ (±1) eu. Such values are somewhat unusual for the associative mechanism for the carbonyl substitution process.[9,10]

Although these data for the equimolar complex/ligand concentrations are fully consistent with second-order kinetics and thus an associative mechanism, under pseudo-first-order conditions plots of k(apparent) versus [ligand] indicated the substitution chemistry was more complex at high ligand concentrations. We have not analyzed this in detail.

2. Reaction of $[Fe_2(CO)_5\{P(OMe)_3\}\{\mu\text{-}C_2(CF_3)_2S\}]$ (2) with $P(OMe)_3$. The kinetics for the substitution of CO by $P(OMe)_3$ in $[Fe_2(CO)_5\{P(OMe)_3\}\{\mu\text{-}C_2(CF_3)_2S\}]$ (**2**) were also examined when a stoichiometric amount of trimethylphosphine was added to **2** (eq 2). Again these

$$[Fe_2(CO)_5\{P(OMe)_3\}\{\mu\text{-}C_2(CF_3)_2S\}] + P(OMe)_3 \rightarrow \underset{\mathbf{2}}{} \quad [Fe_2(CO)_4\{P(OMe)_3\}_2\{\mu\text{-}C_2(CF_3)_2S\}] + CO \quad (2)$$
$$\mathbf{3}$$

reactions obeyed second-order kinetics, as shown by the linear plots of $100/(100 - x)$ (where x is the percentage of **3**) vs time. The rate constants are given in Table II. Derived activation parameters (Table III), $\Delta H^{\ddagger} = 32$ (±1.5) kcal mol^{-1} and $\Delta S^{\ddagger} = 7.3$ (±1) eu, are similar to those calculated for reaction 1. These values are again high and unusual for an associative process such as that determined for reaction 2.

Dynamic NMR Studies. Variable-temperature ^{19}F, $^{31}P\{^1H\}$, and $^{13}C\{^1H\}$ NMR spectra of substituted complexes **2–5**, **7**, **12**, and **14** as well as those of the unsubstituted cluster **1** were recorded. It appears that the line shapes

(9) Bunnett, J. F. In *Investigation of Rates and Mechanisms of Reactions*; Techniques of Chemistry VI; Weissberger, Ed.; Wiley-Interscience: New York, 1974.
(10) Basolo, F.; Pearson, R. G. *Mechanisms of Inorganic Reactions*, 2nd ed.; Wiley-Interscience: New York, 1967; pp 129, 474–477.

Table I. Temperature Dependence of k for CO Substitution by $P(OMe)_3$ on 1 (0.17 M) in Toluene-d_8

temp, K	10^4k, Lmol^{-1} s^{-1}	temp, K	10^4k, Lmol^{-1} s^{-1}
373	0.97(0.05)[a]	388	5.62(0.3)
378	2.01(0.1)	393	9.09(0.45)
383	3.47(0.2)		

[a] Values in parentheses represent one standard deviation.

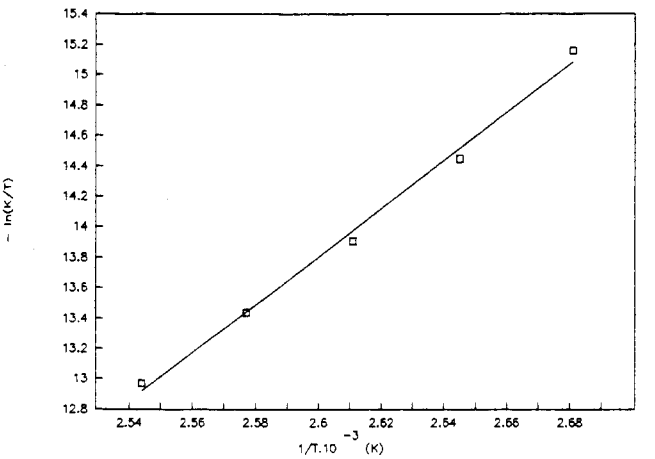

Figure 2. Plot of $-\ln(k/T)$ vs $T^{-1} \times 10^{-3}$ for reaction of **1** with $P(OMe)_3$.

Table II. Temperature Dependence of k for the Substitution of CO by $P(OMe)_3$ on 2 (0.17 M) in toluene-d_8

temp, K	10^4k, Lmol^{-1} s^{-1}	temp, K	10^4k, Lmol^{-1} s^{-1}
383	2.26(0.1)[a]	396	9.97(0.5)
388	4.13(0.2)	398	11.85(0.6)
393	6.50(0.3)		

[a] Values in parentheses represent one standard deviation.

Table III. Eyring Plot Data[a] for the Reaction between 2 and $P(OMe)_3$

$10^{-1}T^{-1}$	$\ln(k/T)$	$10^{-1}T^{-1}$	$\ln(k/T)$
26.11	−14.34	25.25	−12.89
25.77	−13.75	25.12	−12.72
25.44	−13.31		

[a] $\Delta H^{\ddagger} = 32$ (±1.5) kcal mol^{-1}; $\Delta S^{\ddagger} = 7.3$ (±1) eu.

in these spectra are temperature-dependent and clearly indicate averaging of the low-temperature resonances with increasing temperature, implying that fluxional processes are operative in solution. All the line-shape changes throughout the temperature range were found to be completely reversible. Experiments using a wide range of concentrations of the complexes were conducted to confirm that these fluxional processes are intramolecular.

1. Fluxional Behavior of Compound 1. Before we describe the dynamic behavior of selected compounds of the $[Fe_2(CO)_{6-n}L_n\{\mu\text{-}C_2(CF_3)_2S\}]$ type (L = P donor ligands), we report that of the unsubstituted cluster.[1] The variable-temperature $^{13}C\{^1H\}$ NMR spectra of **1** are shown in Figure 3. The spectrum (~190 K) shows four signals with a 1:3:1:1 area ratio. We assigned the area 3 signal to the Fe(1) carbonyl carbons, and we assumed that there is localized interchange of these carbonyl groups on Fe(1).[1] Up to 298 K the resonances of **1** are sharp. As the temperature increases, a broadening of the three signals assigned to the carbonyls bound to Fe(2) is observed and these collapse at about 345 K ($\Delta G^{\ddagger} = 16.4 \pm 0.3$ kcal mol^{-1}). At higher temperatures a broadening of all the signals occurs before they eventually collapse at about 358 K to a broad resonance at δ 206.3. Of particular interest is the

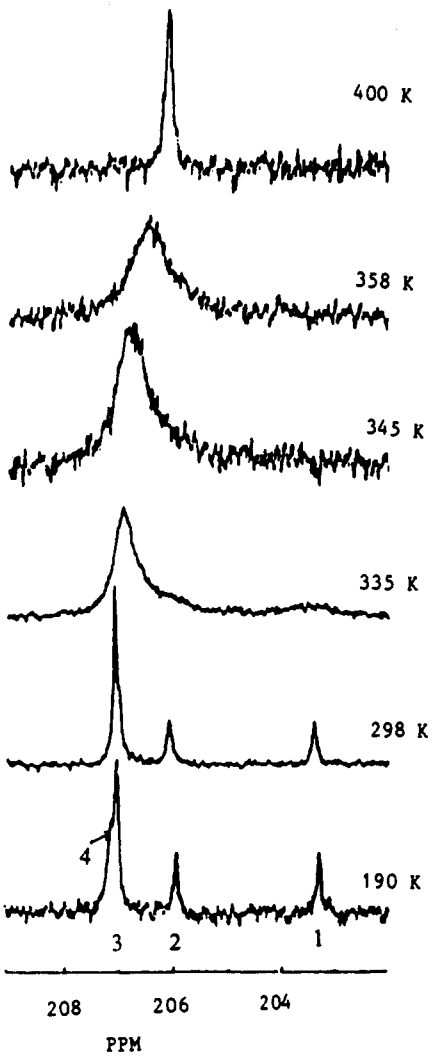

Figure 3. Variable-temperature $^{13}C\{^1H\}$ (CD_2Cl_2 (T = 190 K), $CDCl_3$ (T = 298 K), $C_6D_5CD_3$ (T = 335–400 K); carbonyl region) NMR spectra of **1**: (1) C(10); (2) C(8); (3) C(5), C(6), C(7); (4) C(9).

fact that there is only one signal above 358 K; this means that the high-energy fluxional process ($\Delta G^{\ddagger} \approx 17.2 \pm 0.3$ kcal/mol) involves the (CF_3)—C═C—(CF_3)—S bridging ligand and presumably involves the formation of a mirror plane between Fe(1) and Fe(2).[1] If only localized scrambling of CO on Fe(1) and Fe(2) were occurring at the higher temperature, there should be two observable carbonyl signals. This observation is in accordance with that reported by Hickey et al.[11] for $[Fe(CO)_3\{\overline{Fe(CO)_3}\text{-}\overline{CPh}\text{-}\overline{CPh}\text{-}S\}]$, which is closely related to **1**. However, the exchange process appears at higher temperature in **1**; such a difference must be related to the different substituents on the alkyne.

2. Fluxional Behavior of the Monosubstituted Compound 2. The ^{19}F, ^{13}C, ^{31}P, and ^{13}C NMR spectra of **2** show signals consistent with the presence of two isomers in equilibrium in solution. **2a** is the predominant isomer in solution. The **2a:2b** ratio is not affected by the temperature but depends on the solvent: $CDCl_3$, **2a:2b** = 1.56; CD_3OD, **2a:2b** = 2.03; CD_3CN, **2a:2b** = 2.22. The ^{13}C NMR data in the carbonyl region are given in Table IV, and the assignments to individual carbonyls have been made mainly on the basis of couplings to the phosphorus atom and of chemical shifts.[1]

Table IV. ^{13}C NMR Parameters for $[Fe_2(CO)_{6-n}\{P(OMe)_3\}_n\{\mu\text{-}(CF_3C_2(CF_3)S\}]$ (2, n = 1; 3, n = 2)

	chem shift,[b] ppm			J_{C-P}, Hz		
reson[a]	**2a**	**2b**	**3**	**2a**	**2b**	**3**
5						
6	213.5	209.7	216.8	29		22.5
7	210.5		213.2	30.5		33
8	209.5	209.9	212.2		26.5	24
9	209.2					
10	205.8	206.8	208.2		16	12.5

[a] See Figures 1 and 2 and Chart II. [b] Conditions: room temperature, $CDCl_3$.

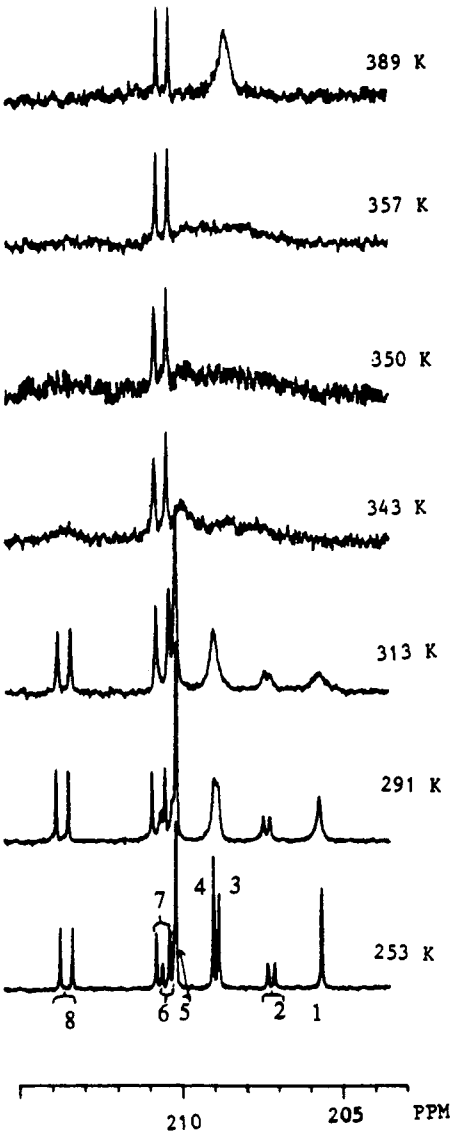

Figure 4. Variable-temperature $^{13}C\{^1H\}$ ($CDCl_3$ (T = 253–291 K), $C_6D_5CD_3$ (T = 313–389 K); carbonyl region) NMR spectra of **2**: (1) C(10), **2b**; (3) C(8) or C(9), **2a**; (4) C(9) or C(8), **2a**; (5) C(5), C(6), C(7), **2b**; (6) C(8), **2b**; (7) C(7), **2a**; (8) C(6), **2a**.

The variable-temperature ^{13}C NMR spectra of **2** are represented in Figure 4. Considering first the spectrum at 253 K, the signal at 209.7 ppm which was assigned[1] to the CO ligands of the $Fe(1)(CO)_3$ unit (**2b**) is sharp; this observation points to a fast local carbonyl-exchange process. Decreasing the temperature below 253 K does not change the spectrum, but the minimum useful temperature was 183 K; below this limit the complex

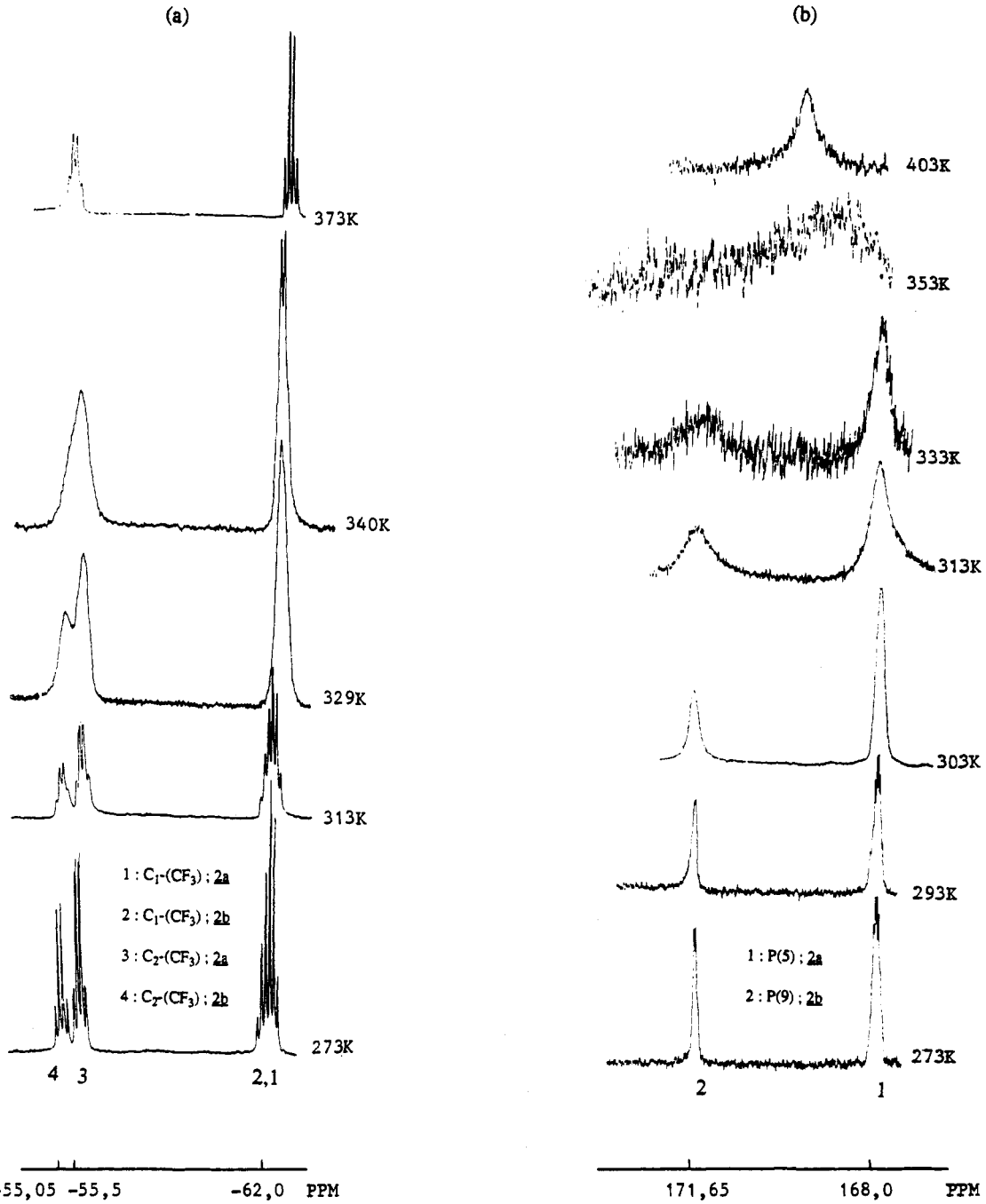

Figure 5. Variable-temperature NMR spectra of **2**: (a) ^{19}F ($C_6D_5CD_3$); (b) ^{31}P ($C_6D_5CD_3$).

precipitated. Up to 253 K the resonances of **2a** as well as those of **2b** are sharp. As the temperature is increased, the two signals of the high-fixed doublet at 206.8 ppm (J_{C-P} = 16 Hz), which was assigned to C(10)O of the minor isomer,[1] average to a singlet at about 320 K. Similarly, the two peaks of the low-field doublet at 213.5 ppm (J_{C-P} = 29 Hz), which were assigned to C(6)O of the major isomer,[1] are observed to coalesce as the temperature is raised to 343 K. At 291 K, the three inequivalent terminal CO's attached to the Fe(2) atom in **2a** show an incipient broadening, and the weighted average peak of their resonances is observed at 208.2 ppm (T_c = 350 K). Above 313 K broadening of most of the resonances occurs, leading to the high-temperature spectrum at 389 K, which consists of a doublet at 209.8 ppm ($J_{C-P} \approx$ 29 Hz) and a broad singlet at 207.8 ppm in a integral ratio of 2:3; the doublet was confirmed by running the spectra at different field strengths. This observation implies that all the carbonyl ligands take part in the local CO exchange processes on the two iron atoms. The ligand dynamics in **2a** partially differs from that reported for $[Fe_2(CO)_5(PPh_3)\{\mu\text{-}C_2(Ph)_2S\}]$.[11] Indeed, the high-temperature (303 K) ^{13}C NMR spectrum of the phenyl derivative showed three CO signals in a 1:1:3 area ratio; the two unit area resonances exhibited ^{31}P–^{13}C coupling, which suggests that there is a localized interchange of carbonyls on the $Fe(CO)_3$ group only.

The dynamic behavior of the ligands in the monosubstituted derivatives **2** was also examined by the temperature dependence of the ^{19}F and ^{31}P NMR spectra. The limiting ^{19}F NMR spectrum of **2** (Figure 5) at 273 K shows four sets of resonances in an integral ratio of 1:1.56:1:1.56 at δ −55.0, −55.5, −61.5, and −62.0. The first two signals

(11) Hickey, J. P.; Huffman, J. C.; Todd, L. J. *Inorg. Chim. Acta* **1978**, *28*, 77.

were assigned to the CF_3 units attached to the C(2) atoms, and the signals at −61.8 and −62.0 ppm were attributed to the CF_3 groups attached to the C(1) atoms[1] of **2b** and **2a**, respectively. When the solution is warmed, the fluorine signals broaden more or less simultaneously and finally merge to two broad resonances at 340 and 329 K. The observed chemical shifts of δ −55.3 and −61.95 for the two signals are in good agreement with the weight-average chemical shifts of the CF_3 units attached to the C(2) and C(1) atoms, respectively. This exchange process observed in variable-temperature ^{19}F NMR spectra is confirmed by the ^{13}C NMR spectra, which clearly show that the two signals at 136.5 and 138.9 ppm, which were assigned[1] to the quaternary C(2) atoms of **2a** and **2b**, respectively, coalesce when the temperature of the solution is raised, to form a signal at δ 137.5 (360 K). Moreover, the ^{31}P–^{13}C couplings ($J \approx 16$ Hz) disappear at 318 K ($\Delta G^{\ddagger} = 16.4 \pm 0.3$ kcal mol^{-1}) and 323 K ($\Delta G^{\ddagger} = 17.3 \pm 0.3$ kcal mol^{-1}) for the minor and the major isomers, respectively. The limiting ^{31}P NMR spectrum in Figure 5b of **2** shows two multiplets at 168.0 and 171.65 ppm with a relative ratio of 1.56:1 at 273 K. The resonance at lowest field (δ 171.65) was assigned to P(9) (**2b**); the other phosphorus atom P(5) (**2a**) was associated with the resonance at δ 168.0.[1] As the temperature is increased to 293 K, the P(5) resonance at 168.0 ppm remains essentially unchanged, whereas that at δ 17.65 transforms into a singlet, a consequence of the disappearance of the ^{31}P–^{19}F coupling. The disappearance of the ^{31}P–^{19}F coupling of the P(5) resonance is only observed at 313 K. As the temperature is raised to 333 K, the two signals broaden and finally coalesce into a single broad resonance at 356 K at ∼169 ppm, which represents the weighted-average chemical shift of the two phosphorus ligands.

From these experimental results the following conclusions can be drawn for compound **2** in solution: (1) complex **2** exists as the two isomers **2a** and **2b**; (2) the main fluxional processes which are detected involve (i) localized scrambling of carbonyl groups on Fe(1) at low temperature (**2b**), (ii) disappearance of ^{31}P–^{13}C and ^{31}P–^{19}F couplings, and (iii) interconversion of the two isomers **2a** and **2b**.

The activation barriers of the observed dynamic processes are then estimated from either the chemical shift differences $\Delta\nu$[12] or the coupling constants J[13] and from the coalescence temperatures of the carbonyl, quaternary carbons, fluorine, and phosphorus signals, respectively, in the ^{13}C, ^{19}F and ^{31}P spectra. Data are summarized in Table V.

3. Fluxional Behavior of the Monosubstituted Complexes 7 and 12. As reported previously,[1] the NMR spectra of **7** and **12** show the existence of two solution isomers **a** and **b**. The **a**:**b** ratios are temperature-independent but change with the solvent ($CDCl_3$, **a**:**b** = 47:53; CD_3CN, **a**:**b** = 54:46). The variable-temperature ^{19}F spectra show that the two resonances which are assigned to the CF_3 groups attached to C(1) (δ −59.5 (**7a**), −60.45 (**7b**); δ −59.75 (**12a**), −60.65 (**12b**)) collapse at 341 K to an averaged multiplet at δ −60.0 (**7**) or −60.2 (**12**), while the two resonances attributed to the CF_3 groups attached to C(2) (δ −55.9 (**7a**), −53.7 (**7b**); δ −55.75 (**12a**), −53.8 (**12b**)) collapse to a multiplet at δ −54.7 (**7**, **12**). Activation barriers are estimated from the coalescence temperatures of the CF_3 signals (Table V).

Table V. Summary of Dynamic $^{13}C\{^1H\}$, ^{19}F, and $^{31}P\{^1H\}$ NMR Data

compd	reson	T_c, K[a]	$\Delta\nu$,[b] Hz	J,[c] Hz	$\Delta G^{\ddagger}(T_c)$,[d] kcal mol^{-1}
2a	Fe(2)–*C*O	350	∼173		16.4
	C(6)O	343		29	17.3
	C(2)	323		6.5	17.3
	P(5)	313		2.6	17.3
2b	*C*(10)O	320		16	16.4
	C(2)	318		16	16.4
	P(9)	293		1.5	16.4
2a ↔ 2b	C(2)	360	192		17.2
	C(1)(*C*F_3)	329	17		17.3 (**a** → **b**)
	C(2)(*C*F_3)	340	41		17.0 (**b** → **a**)
	P(5)–*P*(9)	356	155		17.2 (**a** → **b**)
7a ↔ 7b	C(1)(*C*F_3)	341	79		16.5 (**a** → **b**)
	C(2)(*C*F_3)	353	183		16.5 (**b** → **a**)
12a ↔ 12b	C(1)(*C*F_3)	340	80		16.5 (**a** → **b**)
	C(2)(*C*F_3)	353	179		16.5 (**b** → **a**)
3	*P*(9)	293		2.0	16.4
	P(5)	319		3.3	17.4
	P(5)–*P*(9)	363	126		17.4
	C(10)O	310		12.5	16.1
4a ↔ 4b	C(1)(*C*F_3)	358	38		18.5 (**a** → **b**)
	C(2)(*C*F_3)	366	58		18.0 (**b** → **a**)
	P(5)(OMe)$_3$–*P*(9)-(OMe)$_3$	373	119		18.5 (**a** → **b**)
	P(9)Me$_3$–*P*(5)Me$_3$	383	215		18.0 (**b** → **a**)
14a ↔ 14b	C(1)(*C*F_3)	363	111		17.4 (**a** → **b**)
	C(2)(*C*F_3)	365	122		18.0 (**b** → **a**)
5a ↔ 5b	C(2)(*C*F_3)	330	32		16.6 (**b** → **a**)
		330	32		17.6 (**a** → **b**)

[a] Coalescence temperature. [b] Frequency difference between resonances of exchanging groups in low-temperature limit. [c] Coupling constant. [d] Highest error limit: ±0.8 kcal mol^{-1}.

4. Fluxional Behavior of the Disubstituted Compounds 3, 4, and 14. Spectral data indicate that the single species **3** is present in solution.[1] The fluxional behavior of the ligands in **3** in solution was examined by variable-temperature ^{13}C and ^{31}P NMR studies. The ^{13}C NMR spectrum of this complex, in the carbonyl region, recorded at various temperatures is shown in Figure 6. The limiting spectrum consistent with the structure of **3** was obtained at 273 K. Four resonances are visible at this temperature, and their assignments are quoted in Figure 6. Each of them is split by the phosphorus atom of the $^{31}P(OMe)_3$ ligand ($^2J_{^{31}P-^{13}C}$ = 12.5–33 Hz; see Table IV), indicating that both iron atoms are attached to one phosphite ligand. As the temperature is raised from 273 to 310 K, the resonance due to C(10)O starts to broaden, suggesting that a localized scrambling of the CO ligands at Fe(2), with consequential disappearance of J_{P-C}, takes place. On further warming, the remaining CO resonances also broaden, and finally at 368 K, the spectrum exhibits an average signal, split by the phosphorus atom of the $^{31}P(OMe)_3$ ligands, indicating that a second fluxional process involves intramolecular ligand scrambling. At higher temperatures, the resonance is sharp and $^2J_{^{13}C-^{31}P}$ was estimated to be ∼28 Hz. Beyond 368 K only one CO resonance is observed.

The ^{31}P NMR of **3** at 253 K consists of two resonances: a quartet at δ 176.85 (J_{P-F} = 2 Hz) and a quartet at δ 173.8 (J_{P-F} = 3.3 Hz). It can be seen from Figure 7 that as the sample is warmed from 253 to 319 K differential broadening of the two quartets is observed; this is concomitant with the disappearance of $J_{P(9)-F}$ and $J_{P(5)-F}$, giving $\Delta G^{\ddagger}_{293}$ = 16.3 kcal mol^{-1} and $\Delta G^{\ddagger}_{319}$ = 17.4 kcal mol^{-1} (Table V)

(12) (a) Gutowsky, H. S.; Holm, C. H. *J. Chem. Phys.* **1956**, *25*, 1228. (b) Shanan-Atidi, H.; Bar-Eli, K. H. *J. Chem. Phys.* **1970**, *74*, 961. (c) Sandström, J. *Dynamic NMR Spectroscopy*; Academic Press: London, New York, 1982.

(13) Sanders, J. M. K.; Hunter, B. K. *Modern NMR Spectroscopy*; Oxford University Press: Oxford, U.K., 1988.

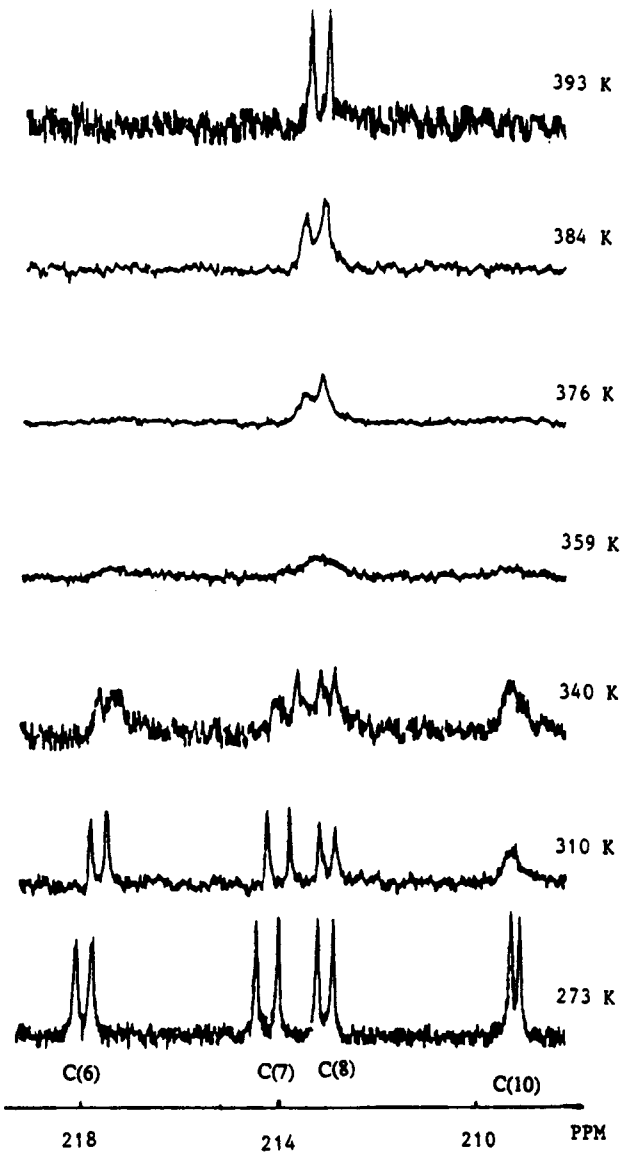

Figure 6. Variable-temperature ^{13}C NMR spectra of **3** (T = 273 K, $CDCl_3$; T = 300–393 K, $C_6D_5CD_3$).

for the fluxional processes, respectively. The activation barriers to remove $J_{P(9)-F}$ and $J_{P(5)-F}$ are similar to that observed for the monosubstituted complex **2**. On further warming, the two resonances assigned to $P(9)(OMe)_3$ and $P(5)(OMe)_3$ collapse at 363 K to an averaged broad singlet. The activation barrier is estimated from the observed coalescence temperature (Table V) and is identical with that obtained for the loss of $J_{P(5)-F}$. This is consistent with a single mechanism for the two fluxional processes.

^{19}F and ^{31}P NMR spectra of **4** show evidence for two isomers[1] in solution. In the major cluster **4a** (67% in $CDCl_3$), the Fe-bound trimethylphosphine occupies the site (9) (Chart II).[1] The variable-temperature ^{19}F NMR spectra for **4** are shown in Figure 8. At room temperature there are four well-resolved split quartets due to **4a** (ca. 67%) (δ −54.05 (J_{F-F} = 8.5 Hz; J_{P-F} = 3.0 Hz); δ −59.95 (J_{F-F} = 8.5 Hz; J_{P-F} = 1.6 Hz)) and **4b** (ca. 33%) (δ −54.55 (J_{F-F} = 8.5 Hz; J_{P-F} = 3.0 Hz); δ −59.25 (J_{F-F} = 8.5 Hz; J_{P-F} = 1.5 Hz)). Resonances due to **4a** and **4b** broaden considerably on raising the temperature, and at 358 K the two signals of the CF_3 groups bound to C(2) atoms collapse to a broad quartet; on further increase of the temperature to 366 K, the two resonances of the CF_3 groups bound to C(1) atoms also collapse. This suggests that **4a** and **4b**

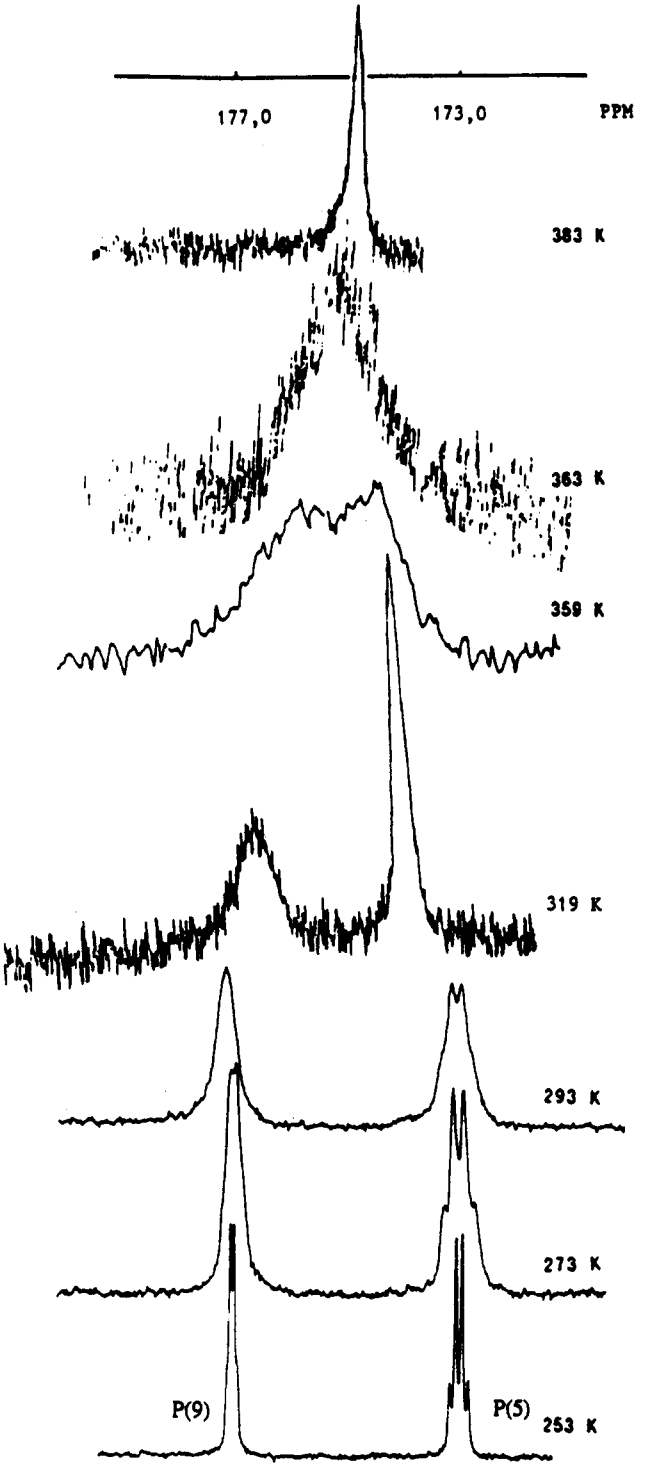

Figure 7. Variable-temperature $^{31}P\{^1H\}$ NMR spectra of **3** (T = 253 K, CD_2Cl_2; T = 273 K, $CDCl_3$; T = 293–383 K, $C_6D_5CD_3$).

exchange with each other. The room-temperature ^{31}P NMR spectrum of **4** shows two resonances at about δ 176 (**4a**, 174.7 (s); **4b**, 177.7 (s)) and −17 (**4a**, −14.65 (s); **4b**, −19.9 (s)), which are assigned to $P(OMe)_3$ and PMe_3, respectively. The former resonances are observed to coalesce as the temperature is raised to 373 K, whereas the latter resonances coalesce at 383 K. This result confirms the fluxional process observed in ^{19}F NMR spectroscopic studies, and from band-shape analysis we estimate a $\Delta G^{\ddagger}$ value of 18.5 (±0.3) kcal mol^{-1} for the **4a** → **4b** process and 18.0 (±0.3) kcal mol^{-1} for the **4b** → **4a** one.

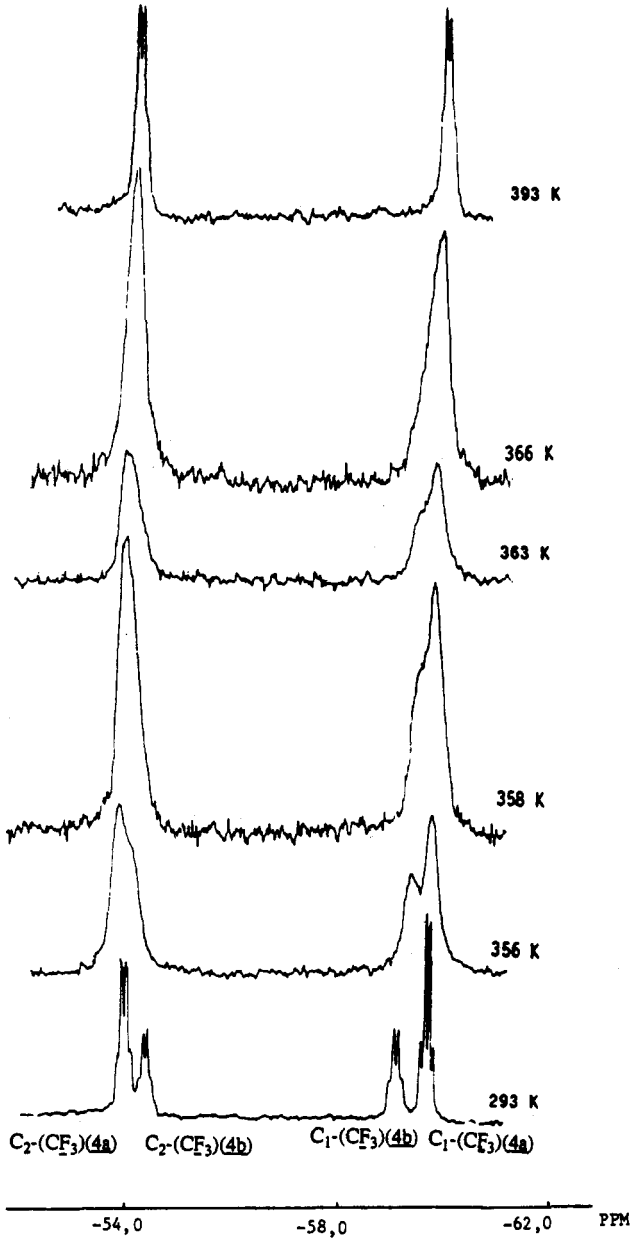

Figure 8. Variable-temperature ^{19}F NMR spectra of 4.

Chart II

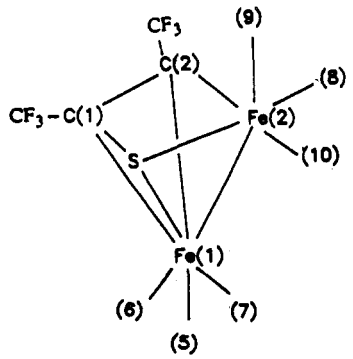

There is spectral evidence (^{13}C, ^{19}F, ^{31}P NMR)[1] for two isomers of **14** in solution. In these isomers **14a** and **14b** the (diphenylphosphino)ethane ligands chelate the Fe(1) atom (in "P(5)–P(6)" positions) or the Fe(2) atom (in "P(9)–P(10)" positions), respectively (see Chart I). The major isomer is **14b** ($CDCl_3$, 68%; CD_3CN, 79%). The dynamic behavior of the ligands in the disubstituted derivative **14** was examined by the temperature dependence of the ^{19}F NMR spectra (Figure 9). Separate resonances are observed for the CF_3 groups of the two isomers, at room temperature. As the temperature is raised to 363 K, the pair of low-field resonances, assigned to the CF_3 units attached to C(1) atoms, gradually broaden and merge into a broad resonance at −54.2 ppm, while the pair of high-field resonances, which are assigned to the CF_3 units attached to the C(2) atoms, coalesce to a broad singlet at a slightly higher temperature (365 K). The fluxional process involves the interconversion of **14a** and **14b** with $\Delta G^{\ddagger}_{a\rightarrow b} = 17.4$ (±0.3) kcal mol^{-1} and $\Delta G^{\ddagger}_{b\rightarrow a} = 18.0$ (±0.3) kcal mol^{-1}.

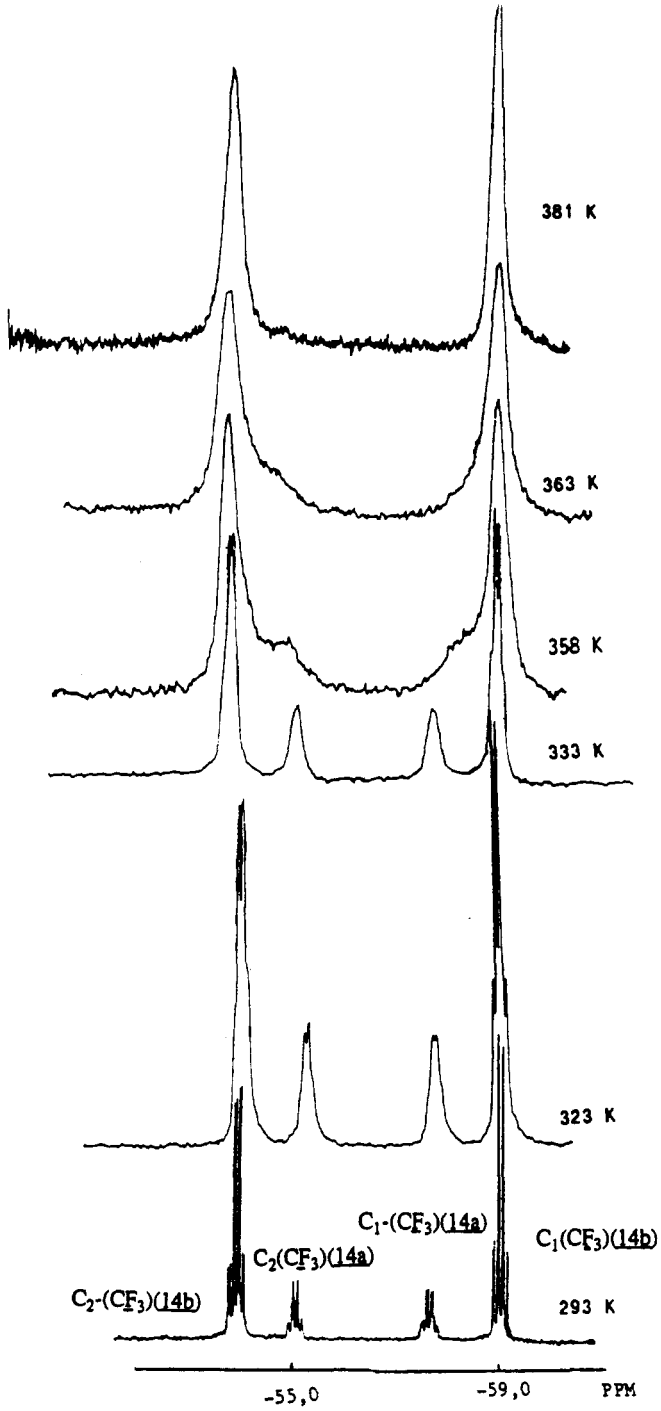

Figure 9. Variable-temperature ^{19}F NMR spectra of **14**.

5. Fluxional Behavior of the Trisubstituted Compound 5. The trisubstituted cluster **5** exists as a mixture of the isomers **a** and **b** (Chart I), as shown by its NMR data.[1] These isomers rapidly isomerize on the NMR time

scale at elevated temperatures. From variable-temperature ^{19}F spectroscopic studies a free enthalpy of activation of 17.6 ($\Delta G^{\ddagger}_{a\rightarrow b}$) and 16.6 kcal mol^{-1} ($\Delta G^{\ddagger}_{b\rightarrow a}$) can be estimated.

Discussion

Mechanisms of CO Substitution in the Clusters. The reactions under consideration are the substitution of $P(OMe)_3$ for CO in both $[Fe_2(CO)_6\{\mu\text{-}C_2(CF_3)_2\}]$ (1) (reaction 1) and $[Fe_2(CO)_5\{P(OMe)_3\}\{\mu\text{-}C_2(CF_3)_2S\}]$ (2) (reaction 2). In reaction 2 the disubstituted complex 3 is obtained by a process which seems to obey the empirical rule of one carbonyl replacement at each metal center[14] under thermal activation. Our kinetic results concerning these reactions rule out a dissociative substitution pathway for these compounds and establish the associative nature of the substitution process. The assignment of an associative mechanism is supported by the fact that no modification of the kinetics of the substitution reactions is observed when the experiment is conducted under a CO atmosphere in the NMR tube. Eighteen-electron binary metal carbonyls generally react by a dissociative process; however, the associative mechanism may become possible if particular ligands in the complexes can accept a pair of electrons from the metal.[6a] Such ligands are present in 1 and in 2. Thus, the replacement of carbon monoxide in eq 1 involves three prior bond scissions and the formation of new bonds to expose a coordinatively unsaturated 16-electron iron center, which is followed by the rapid association with the nucleophile to afford the substituted product. This stepwise sequence is depicted in Scheme I coupled to the subsequent isomerization of the cluster. As proposed, the process does not involve the formation of a 20-electron intermediate.

A similar mechanism is suggested for the replacement of CO in eq 2, and the rate constants and the activation values are very close for both systems. This indicates that the presence of the first nucleophile ($P(OMe)_3$) at an iron site has only limited electronic and steric effects on the second incoming nucleophile which coordinates the other iron atom.

The values of the activation enthalpy ($\Delta H^{\ddagger} \approx 31$ kcal mol^{-1}) are high compared with those of other binuclear or cluster metal carbonyls.[15] Moreover, the slightly positive value of the activation entropy is unusual for an associative mechanism.[9] This suggests that for S_N2 of 1 and 2 there is more bond breaking than bond making in the formation of the active intermediate A,[6a,16] as shown in Scheme I. Such a positive entropy is also observed when carbon monoxide is replaced by phosphine or phosphite ligands in $[Fe_3Cp(CO)_3(\mu_3\text{-}CO)(\mu\text{-}CO)(\mu_3,\eta^2(\|)\text{-}CF_3C_2CF_3)]$ according to an associative path.[17] The associative process suggested for the exchange of CO by trimethyl phosphite in 1 and 2 under thermal conditions contrasts with the dissociative nature of this reaction under electrochemical activation.[1] The results illustrate once again that electrochemically and thermally activated substitution reactions can follow two different pathways.[18] This is due to the fact that carbonyl loss occurs readily at the electrogenerated 19-electron metal center,[1] thus making the substitution process associative in nature.

Scheme I[a]

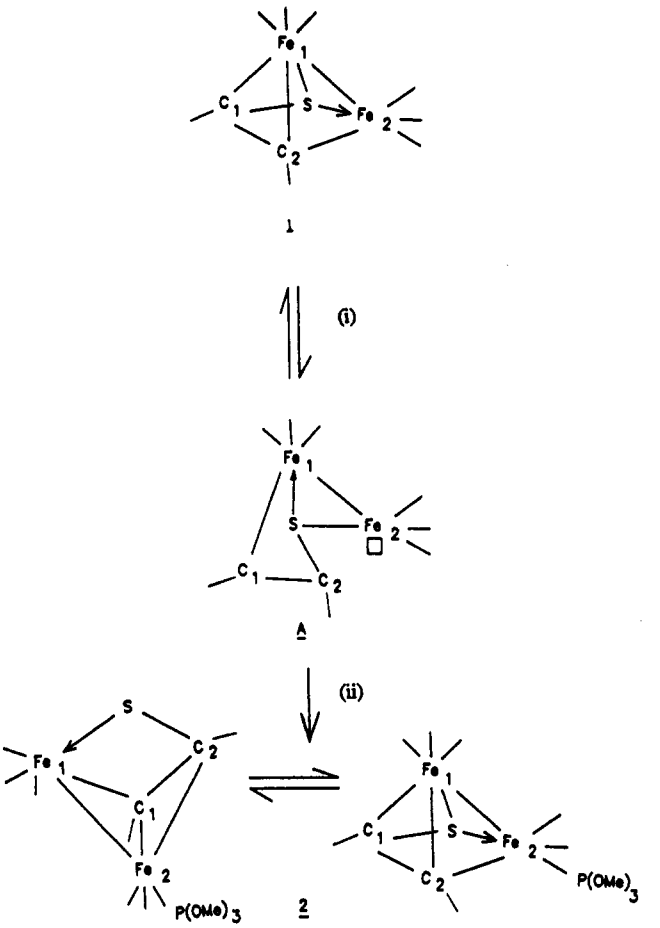

[a] Legend: (i) (a) $C_{(2)}$–$Fe_{(2)}$, $C_{(2)}$–$Fe_{(1)}$ and $C_{(1)}$–S bond cleavage, (b) $C_{(2)}$–S bond formation; (ii) (c) $C_{(1)}$–$Fe_{(2)}$ or $C_{(2)}$–$Fe_{(1)}$ and $C_{(2)}$–$Fe_{(2)}$ bond formation, (d) –CO, (e) $+P(OMe)_3$.

NMR and Intramolecular Exchange. The dynamic behavior of the clusters studied here is provided by the temperature-dependent ^{13}C, ^{19}F, and ^{31}P spectra. We discuss first and mostly the results obtained for the monosubstituted complex 2. The observed exchange behavior can be understood in terms of two-stage ligand motion processes. The low-energy one consists of ligand movements at Fe(2); it involves either the disappearance of ^{31}P–^{13}C and ^{31}P–^{19}F couplings (**2b**) or local CO exchange (**2a**). The high-energy process concerns ligand movements at Fe(1), in concert with rotation of the $C_2(CF_3)_2S$ ligand. Two main hypotheses could be made to rationalize why the P(9)–F, P(9)–C(2), and P(9)–C(10) couplings are removed in the low-energy process. The simplest explanation is to invoke a fast exchange of the phosphite and

(14) Atwood, J. D.; Wovkulich, M. J.; Sonnenberger, D. C. *Acc. Chem. Res.* **1983**, *16*, 350.

(15) The rate law for the mechanism proposed in Scheme I is

$$\frac{d[Fe]}{dt} = -\frac{k_1k_2[Fe][P]}{k_{-1} + k_2[P]}$$

where k_1 and k_{-1} are rate contstants for the first step (Scheme I). Then, k_2 is the rate constant for the following step. The reported rate constants (k_{obsd} of Tables I and II) are $(k_1k_2)/k_{-1}$ or $k_{eq}k_2$, because of low concentrations of $P(OMe)_3$; $r = (k_1k_2/k_{-1})[Fe][P]$. Therefore, as pointed out by a reviewer, the reported activation parameters are the sums of the two steps, which makes their interpretation difficult.

(16) Schneider, J.; Minelli, M.; Huttner, G. *J. Organomet. Chem.* **1985**, *294*, 75.

(17) Robin, F.; Rumin, R.; Pétillon, F.; Talarmin, J. to be submitted for publication.

(18) Lhadi, E. K.; Mahé, C.; Patin, H.; Darchen, A. *J. Organomet. Chem.* **1983**, *246*, C61.

Scheme II[a]

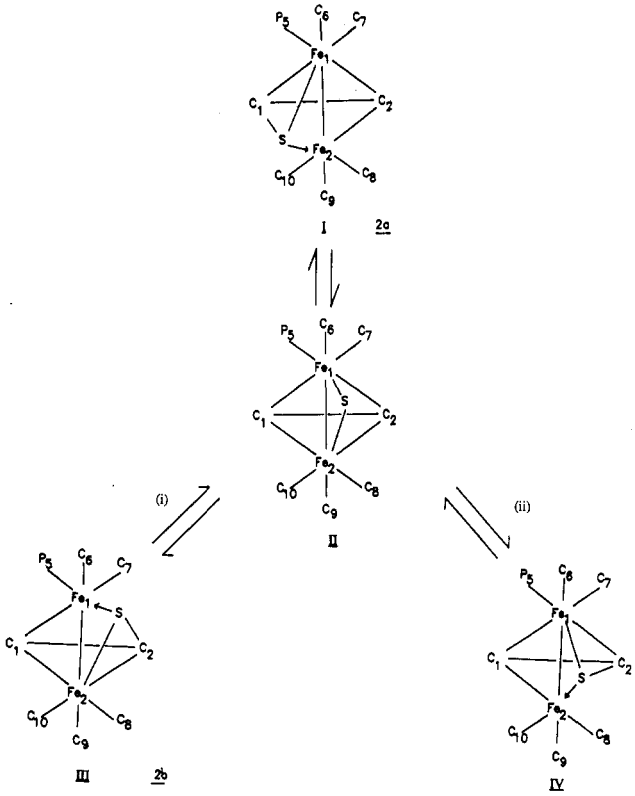

[a] Legend: (i) high-energy process ($C_{(2)}$–$Fe_{(1)}$ bond breaking; $C_{(2)}$–S bond making); (ii) low-energy process ($C_{(2)}$–$Fe_{(2)}$ bond breaking; $C_{(2)}$=S bond making).

carbonyl ligands of the $Fe(2)(CO)_2\{P(OMe)_3\}$ unit on the NMR time scale. The second one is to suggest σ-Fe(2)–C(2) bond breaking. We favor the second assumption for two main reasons. First, the P(9)–C(8) coupling does not disappear concomitantly with that of P(9)–C(10). This difference in the behavior of the two systems must be related to the local environment of C(10) and C(8); the C(10)O and C(8)O ligands are trans and cis to C(2), respectively. Second, the fact that the values of the activation barriers (see Table V) for exchange of the three carbonyls in the $Fe_2(CO)_3$ unit (**2a**) and removal of the P–C and P–F couplings are exactly the same is fully consistent with a single mechanism implying σ-Fe(2)–C(2) bond breaking. The high-energy process is related to interisomer (**2a** ↔ **2b**) exchange. It appears that a common mechanism for CF_3, $P(OMe)_3$, and CO scrambling is likely. Our study suggests that this exchange may occur via an intermediate II, resulting from I (**2a**) (Scheme II) by concerted cleavage of the C(1)–S bond, allowing the sulfur atom to swing around the Fe(1)–Fe(2) axis, and C(1)–Fe(2) bond making. The mechanism proposed for the rearrangement of **2** predicts the exchanges C(1) ↔ C(2), C(6) ↔ C(10), C(5)/P(5) ↔ P(9)/C(9), and C(7) ↔ C(8). The intermediate II is also implied in the low-energy process as shown in Scheme II, which accounts for the observed changes in the NMR spectra.

Now it can be seen from Figure 3 that at 190 K the resonances due to the carbonyl ligands in the parent complex **1** labeled as (5), (6), and (7) (Chart I) have already collapsed, whereas the resonances due to the carbonyl ligands labeled as (8), (9), and (10) remain sharp. This suggests that the activation barrier to localized scrambling within the set of carbonyl ligands associated with the iron atom (Fe(1)) to which the alkyne forms a π-bond is lower than that for the carbonyl ligands associated with the iron atom (Fe(2)) with which the alkyne is σ-bonded. The carbonyl ligands associated with the iron atom having the highest coordination number (Fe(1)) are nonrigid at this temperature, whereas the carbonyl ligands associated with the iron having the lowest coordination number remain rigid. Such a behavior could not be explained here by an argument based on steric effects from the high coordination number as postulated before by Aime et al.[19] Moreover, we can deduce from previously reported data[1] and from Figure 4 that the reaction of trimethyl phosphite with **1** led mainly to the replacement of a carbonyl on the iron atom at which there was scrambling, i.e. Fe(1). This raises the question as to why the thermodynamic product (**2a**) carries phosphite on Fe(1), the metal atom with the higher coordination number and at which there was scrambling at low temperatures. The simplest explanation is to invoke a third low-energy process involving Fe(1)–C(2) bond breaking. This hypothetical movement would happen at a temperature lower than that which could be obtained without precipitation of the complex in the solvents used in the experiments, and thus the process associated with this motion was not observed in the spectra. Such a bond breaking would facilitate the loss of the C(5)O group, which is trans to C(2), and its replacement by a more basic nucleophile. Our NMR data suggest the presence in solution of unsaturated species resulting from iron–carbon bonds breaking. This explains why the complexes studied here apparently react with nucleophiles via an associative mechanism.

The variable-temperature ^{13}C and ^{31}P NMR spectra of **3** are similar to those of **2** and therefore indicate that the exchange processes are of comparable energies (Table V). The observed exchanges involve again the interchange of the bonding functions of the end atoms of the $C_2(CF_3)_2S$ ligand. This process would create a time-averaged mirror plane which is perpendicular to and bisects the Fe–Fe bond; therefore, the $Fe(CO)_2\{P(OMe)_3\}$ units become equivalent under this condition. The similarity of the variable-temperature ^{19}F and ^{31}P spectra of **7**, **12**, **4**, **14**, **5**, and **2** suggest that the exchange processes are comparable in all of these complexes and are fully consistent with a single isomerization mechanism as described in Scheme II.

It appears that neither the extra bulkiness of the phosphite, phosphine, and diphosphine ligands nor their basicity raises significantly the activation energy of the carbonyl and $C_2(CF_3)_2S$ ligand exchange processes. However, we note a slight effect of the more basic PMe_3 relative to $P(OMe)_3$ when we compare the activation barriers of the disubstituted complexes **3** and **4** (Table V). These results contrast with those obtained by Huttner et al.[20] for the closely related complex $[Fe(CO)_2L\{Fe(CO)_2L\text{-}CH\text{-}CPh\text{-}S\}]$ (L = $P(OMe)_3$), for which the rapid exchange between the two iron centers' energy (~13.4 kcal mol^{-1}) is quite low and differentiates strongly from that observed in the parent complex; a steric effect may be responsible for this behavior.

Summary

Substitution of carbon monoxide by trimethyl phosphite under thermal activation in the diiron complex [Fe_2-

(19) Aime, S.; Milone, L.; Sappa, E. *Inorg. Chim. Acta* **1976**, *16*, L7.
(20) Fässler, T.; Huttner, G. *J. Organomet. Chem.* **1990**, *381*, 391.

$(CO)_6\{\mu\text{-}C_2(CF_3)_2\}$] (1) takes place by an associative substitution mechanism. The presence of this pathway in the complex may be attributed to the delocalization of a pair of electrons from the metal complex onto the bridging ligand $C_2(CF_3)_2S$, making a vacant low-energy orbital available on the metal which is accessible to nucleophilic attack.

Our variable-temperature NMR results provide information on the isomerization behavior of phosphite- or diphosphine-substituted derivatives of cluster 1. The barriers for the carbonyl and $C_2(CF_3)_2S$ ligand exchange are almost independent of the nature and the size of the phosphite and phosphine ligands.

Experimental Section

Materials. The carbonyl cluster $[Fe_2(CO)_6\{\mu\text{-}C_2(CF_3)_2S\}]$[21] (1) and the monosubstituted (2 7, 12),[1] disubstituted (3, 7, 12),[1] and trisubstituted (5)[1] products were obtained as reported before.

Deuteriated solvents were degassed and transferred under argon to the reaction tube before use.

Kinetic Measurements. Equilibrium and kinetic studies of the rates of carbonyl substitution were followed by ^{19}F NMR (93.66 MHz), using a JEOL FX 100 spectrometer. The reactions were carried out in oxygen-free toluene-d_8 solutions and under conditions where the concentrations of the cluster and that of trimethyl phosphite or the diphosphine are the same (in a typical experiment, the concentrations were 0.15–0.20 M). The kinetics of the reactions were followed by monitoring the increasing intensity of a typical ^{19}F NMR resonance of the product (2, 3). Plots of $100/(100-x)$ (x = percentage of product vs time (2, 3) were linear. The slopes of these lines gave values of k_{obsd}. One kinetic experiment involving 1 and $P(OMe)_3$ was also carried out under pseudo-first-order conditions with at least a 20-fold excess of nucleophile. This reaction proceeded to completion to give the monosubstituted product 2.

Temperature-Dependent NMR Spectroscopy. ^{13}C NMR spectra were recorded at 75.47 MHz by using a Bruker AC 300 spectrometer. The ^{31}P (40.26 MHz) and ^{19}F (93.66 MHz) spectra were obtained on a JEOL FX 100. The ^{31}P and both ^{13}C and ^{19}F chemical shifts are referenced to external 85% H_3PO_4 and tetramethylsilane, respectively. Positive chemical shifts are to low field of the external standard.

The energies of activations in Table V were calculated according to the procedure given by Shanan-Atidi et al.[12b] The variable-temperature ^{13}C and ^{31}P NMR study allowed the determination of T_c, the coalescence temperature. At this temperature the observed chemical shift was found to be in good agreement with the weighted-average chemical shifts obtained from the slow-exchange spectrum. Through the use of the relative populations of exchanging ligands (CO, CF_3, P) and the coalescence temperature, the activation energy for intramolecular ligand scrambling was calculated.[12]

Acknowledgment. We thank Prof. H. Patin, Prof. A. Darchen (ENSC Rennes), and Dr. C. J. Pickett for helpful discussions. The CNRS and Brest University are acknowledged for financial support.

OM920786C

(21) Rumin, R.; Pétillon, F. Y.; Manojlović-Muir, L.; Muir, K. W. *Organometallics* **1990**, *9*, 944.